A FAR-FIELD RADIO FREQUENCY EXPERIMENTAL EXPOSURE SYSTEM AND 31 DAY EXPOSURE EXPERIMENT ON UNRESTRAINED MICE

A Thesis
Submitted to the Graduate Faculty
of the
North Dakota State University
of Agriculture and Applied Science

By

Jared William Hansen

In Partial Fulfillment of the Requirements
for the Degree of
MASTER OF SCIENCE

Major Department:
Electrical Engineering

November 2015

Fargo, North Dakota

North Dakota State University

Graduate School

Title

A FAR-FIELD RADIO FREQUENCY EXPERIMENTAL EXPOSURE SYSTEM AND 31 DAY EXPOSURE EXPERIMENT ON UNRESTRAINED MICE

By

Jared William Hansen

The Supervisory Committee certifies that this ***disquisition*** complies with North Dakota State University's regulations and meets the accepted standards for the degree of

MASTER OF SCIENCE

SUPERVISORY COMMITTEE:

Dan Ewert
Chair

Roger Green

Ben Braaten

Tom Gustad

Approved:

11/16/15	Scott Smith
Date	Department Chair

ABSTRACT

Many studies have been performed on exploring the effects of radio frequency energy on biological function *in vivo*. In particular, gene expression results have been inconclusive due, in part, to a lack of a standardized experimental procedure. This thesis describes a new far field RF exposure system for unrestrained murine models that reduces experimental error and a 31 day experiment using mice *in vivo*. The experiment uses whole body exposure to continuous RF energy at 2.45 GHz on unrestrained, *in vivo* mice. Using RNA-seq to analyze the entire murine genome, the data is statistically analyzed using combinations and empirical p-values. The analyzed data's genome are explored using Ingenuity Pathway Analysis to locate gene functional groups within heart tissues. Results show an intriguing finding of a discrete/continuous system due to radio frequency energy, along with genes alteration found in heart functional groups.

ACKNOWLEDGMENTS

To the many people that have helped me complete this study, including but not limited to Sumit Gosh, Curt Doetkott, Brandon Stevens, Lauren Singelmann, Sajid Asif, Saeed Khan, Andrew Taylor, Tom Gustad, Roger Green, Ben Braaten, and my advisor Dan Ewert. Without any of you I would not have been able to complete this work.

I also thank the Genome Technology Access Center in the Department of Genetics at Washington University School of Medicine for help with genomic analysis. The Center is partially supported by NCI Cancer Center Support Grant #P30 CA91842 to the Siteman Cancer Center and by ICTS/CTSA Grant# UL1TR000448 from the National Center for Research Resources (NCRR), a component of the National Institutes of Health (NIH), and NIH Roadmap for Medical Research. This publication is solely the responsibility of the authors and does not necessarily represent the official view of NCRR or NIH.

Finally, I thank the North Dakota Department of Commerce for funding from the ND Venture Grant 14-08-J1-66 phase one venture grant.

DEDICATION

I dedicate this work to my parents, Patricia and William Hansen. Both have taught me many things, but the most important being the ability to overcome adversity.

TABLE OF CONTENTS

LIST OF TABLES

LIST OF FIGURES

LIST OF ABBREVIATIONS

RF.....Radio Frequency.

IEEE.....Institute of Electrical and Electronics Engineers.

WHO.....World Health Organization.

SAR.....Specific Absorption Rate.

EM.....Electromagnetic.

qPCR.....Qualitative Polmerase Chain Reaction.

IACUC.....Institutional Animal Care and Use Committee.

GTAC.....Genome Technology Access Center.

TPM.....Transcripts Per Million.

LIST OF SYMBOLS

R.....The distance between the horn antenna and the mice cage.

PrdB .....Power received at the patch antenna.

PRdB.....Power received at the spectrum analyzer.

C_ldB .....Insertion loss for a transmission line.

U_{C_l}.....Uncertainty of the insertion loss.

Pr.....Power received at the patch antenna measure in Watts.

S .....Power Density incident on the patch antenna.

Ae.....Area of the effective aperture.

Dr .....Directivity of the patch antenna.

λ.....Wavelength.

c.....Speed of light.

f .....Frequency in hertz.

U_λ .....Uncertainty of the wavelength.

U_{Ae} .....Uncertainty of the effective aperture.

U_{Dr} .....Uncertainty of the directivity of the patch antenna.

U_{PR} .....Uncertainty of the spectrum analyzer.

T_{PR}.....Tolerance measurement of the spectrum analyzer.

U_S .....Uncertainty of the power density measurement.

PRba.....Power received at the biconical antenna.

U_{PRba} .....Uncertainty of the power received at the biconical antenna.

P_e .....Power absorbed by the patch antenna in an empty enclosure.

P_I .....Input Power.

P_O .....Output Power.

P_R.....Reflected Power.

P_S.....Power absorbed by the patch antenna while a sample is present.

U_{SAR} .....Uncertainty of the SAR measurement.

Gt.....Gain of the horn antenna.

Pt .....Power transmitted from the horn antenna.

PAPER 1. A FAR-FIELD RADIO-FREQUENCY EXPERIMENTAL EXPOSURE SYSTEM WITH UNRESTRAINED MICE[1]

1.1. Introduction

Radio frequency (RF) energy is nearly everywhere, it is used in cell phones, wireless internet and many other RF sources. The RF energy levels used by common devices are below the threshold level which does not produce heating of cells in living tissues. However, this low-level exposure of RF energy has still raised concerns over its possible effects on human health, specifically, genetic alterations. Researchers have investigated if RF energy can induce changes in biological function [3, 6, 8, 11]. The methods used to investigate RF energy effects have varied widely depending on study. This variation in procedures has led to a lack of reproducibility, and because of that, inconclusive results [3, 11]. The goal of this paper is to describe a new experimental exposure system to explore the effects of far-field RF energy on biological function in unrestrained murine models, *in vivo*.

Paffi *et al* [7] performed an extensive review of exposure systems. Many of these used a horn antenna to deliver RF energy, but lack long term continuous exposure for free moving murine models. Other studies including Kesari *et al* [5] and Wasoontarajaroen *et al* [12] used intermittent RF exposure, and still others in Paffi *et al* [7] used a reverberation chamber to deliver RF energy. For this work, an RF amplifier, horn antenna and anechoic chamber material

[1] The material in this chapter was co-authored by Jared Hansen, Sajid Asif, Lauren Singelmann, Muhammad Saeed Khan, Sumit Ghosh, Tom Gustad, Curt Doetkott, Benjamin Braaten, and Daniel Ewert. Jared Hansen worked on the uncertainty analysis, characterization of the test room, experimental specific absorption rate calculation, and radio-frequency exposure experiment. Jared Hansen also drafted and revised all version of this chapter. Sajid Asif worked on the microstrip patch antenna, characterization of the test room, experimental specific absorption rate calculation, and radio-frequency exposure experiment. Lauren Singlemann worked on the characterization of the test room, and radio-frequency exposure experiment. Muhammad Saeed Khan worked on the microstrip patch antenna. Sumit Ghosh, Tom Gustad, Curt Doetkott, Benjamin Braaten, and Daniel Ewert supervised the experiments and provided review feedback.

were used to: 1) provide a more precisely defined RF field for accurate long-term exposure in freely moving test subjects and 2) the uncertainty analysis is more convenient as opposed to a reverberation chamber. This exposure system coupled with uncertainty analysis addresses many of the shortcomings stated in [13].

This paper describes the equipment and materials used, creation of a patch antenna, uncertainty analysis of the equipment, characterization of the background RF energy in the test room, specific absorption rate calculation, and setup of the equipment used for testing far-field RF exposure on unrestrained murine models.

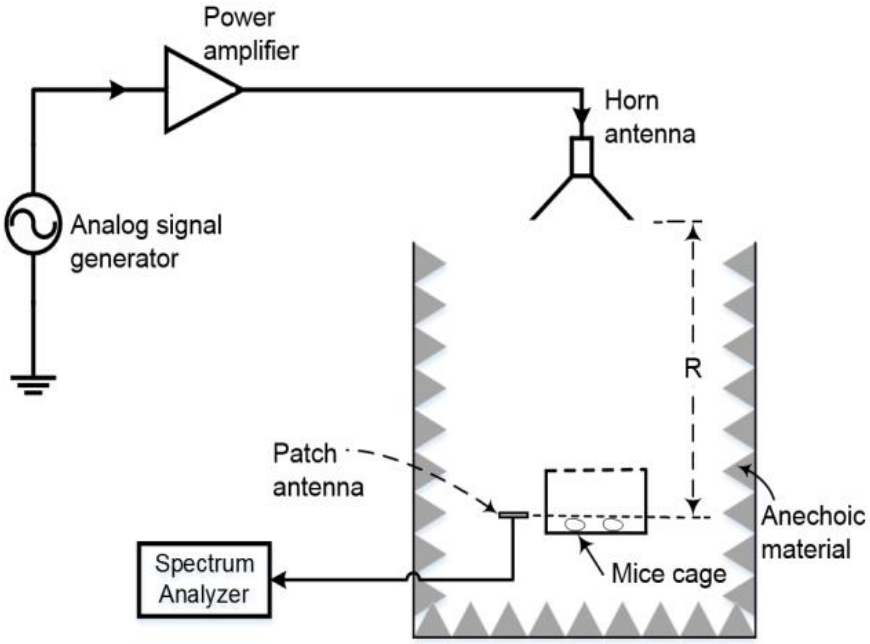

Figure 1. Layout of Experimental Setup. Layout of the experimental setup for RF exposure of mice with all the apparatus used. The transmitter antenna (Horn) is at the distance R from the mice cage.

1.2. Materials and Methods

Figure 1 depicts the experimental setup for the RF exposure system for unrestrained murine models, *in vivo*. The figure shows a horn antenna connected to a power amplifier and signal generator, placed a distance 'R' away from the mice cage. The levels of RF are measured

by a patch antenna connected to a spectrum analyzer. Table 1 lists the equipment used, and the make/model/specifications.

Table 1
Equipment Used

Sr. No.	Name	Make/Model/Specifications
1.	Analog Signal Generator	Agilent/N5181A 100KHz - 3GHz
2.	Spectrum Analyzer	Agilent E4402B 9KHz - 3GHz
3.	Horn Antenna	TDK RF Solutions (HRN-0118) 1-18 GHz
4.	Patch Antenna	Manufactured on TMM4 f = 2.43 GHz, Gain = 4.8 dBi thickness= 1.52mm and 0.5 oz. copper
5.	Biconical Antenna	A.H. Systems (SAS-521-4) 25 MHz – 4 GHz
6.	Coax cable	UTIFLEX Micro-Coax 26.5 GHz
7.	Power Amplifier	Mini-Circuits (ZHL-30W-252-S+) 700 to 2500 MHz
8.	Mouse cage	Plastic (20 x 30 x 16 cm^3)
9.	Anechoic material	MVG AEP-18 (pyramid absorber) 30 MHz – 18 GHz

1.2.1. Uncertainty Analysis of Equipment

The uncertainty analysis of the test equipment was conducted on the equipment used to measure and record the power received by the treatment group. Performing uncertainty analysis on the equipment is an important step because it assists in ensuring that the power levels are below IEEE standard for continuous exposure and helps in comparing the results of RF

experiments [4]. The equipment includes: a patch antenna, two transmission lines, and a spectrum analyzer. With calibrated equipment, the assumption is that the uncertainty and loss data given by each respective data sheet is true. Table 2 shows the uncertainty values given for equipment used by the authors.

Table 2
Uncertainty of Equipment

Equipment	Uncertainty
Biconical Antenna	±1.00 dBm
Coax Cables	±0.01 dBm
Spectrum Analyzer	±0.40 dBm
Horn Antenna	±2.00 dBm
Network Analyzer	±1.30 dBm
Signal Generator	±2.00 Hz

Other uncertainty values (i.e. patch antenna characteristics) were computed using equations 1-12. The power received at the patch antenna is:

$$PrdB=PRdB+2*|C_{l}dB| \tag{1}$$

where PrdB is the power received at the patch antenna, PRdB is the power received at the spectrum analyzer, and C_l is the insertion loss of each transmission line. Because the transmission lines are calibrated we can make the assumption that

$$C_{l}dB=C_{l1}=C_{l2} \tag{2}$$

and the uncertainty of each transmission line is:

$$U_{C_l}=U_{C_{l1}}=U_{C_{l2}}. \tag{3}$$

Next, the power received at the patch antenna can then be converted into watts by:

$$\mathrm{Pr}=10^{\frac{\mathrm{Prdb}}{10}} \quad (\mathrm{W}). \tag{4}$$

Then the power density incident on the antenna can then be calculated using equation 5 from the introduction:

$$\mathrm{S}=\frac{\mathrm{Pr}}{\mathrm{Ae}} \qquad (\mathrm{W/m^2}), \tag{5}$$

where S is the power density and Ae is the area of the effective aperture, computed by:

$$\mathrm{Ae}=\frac{\mathrm{Dr}*\lambda^2}{4\pi}. \tag{6}$$

Dr is the directivity of the patch antenna with an efficiency of 95% and λ (wavelength) and defined by:

$$\lambda=\frac{\mathrm{c}}{\mathrm{f}}, \tag{7}$$

where c is the speed of light in m/s and f is the frequency in hertz. The uncertainty of λ can be computed by

$$\mathrm{U}_\lambda=\sqrt{(\frac{\partial\lambda}{\partial\mathrm{f}}*\mathrm{U}_\mathrm{f})^2}. \tag{8}$$

Then the uncertainty of the effective aperture can be calculated as:

$$\mathrm{U}_{\mathrm{Ae}}=\pm\sqrt{(\frac{\partial\mathrm{Ae}}{\partial\mathrm{Gr}}*\mathrm{U}_{\mathrm{Gr}})^2+(\frac{\partial\mathrm{Ae}}{\partial\lambda}*\mathrm{U}_\lambda)^2}. \tag{9}$$

Now the uncertainty of the power received at the spectrum analyzer can be computed. This value U_{PR} is dependent on the value recorded by the spectrum analyzer (PR) and its respective measurement tolerance ($\mathrm{T_{PR}}$) given by the manufacturer:

$$U_{PR} = \pm \frac{\left| 10^{\frac{PR+T_{PR}}{10}} - 10^{\frac{PR-T_{PR}}{10}} \right|}{2} \text{ (W).} \quad (10)$$

Knowing that the transmission lines are identical the equation can be simplified to:

$$U_{Pr} = \pm \sqrt{(U_{PR})^2 + 2*(U_{C_l})^2}. \quad (11)$$

Knowing the uncertainty for the effective area of the aperture and the power received at the patch antenna. The uncertainty of the power density can be determined as:

$$U_S = \pm \sqrt{\left(\frac{\partial S}{\partial Pr} * U_{Pr}\right)^2 + \left(\frac{\partial S}{\partial Ae} * U_{Ae}\right)^2}. \quad (12)$$

These equations were used for the test equipment and the uncertainty of the power density was calculated. Figure 2 shows the relationship between the power levels of 1-20 dBm and their corresponding power densities. The error bars represent the uncertainty of the power densities. Figure 3 depicts the power levels of 16.5-16.6 dBm (power levels used by the authors) at increments of .005 dBm. Following the continuous RF energy exposure standards set by IEEE, and the uncertainty analysis provided here, power density levels can be set such that they will fall below the exposure maximum allowed [4].

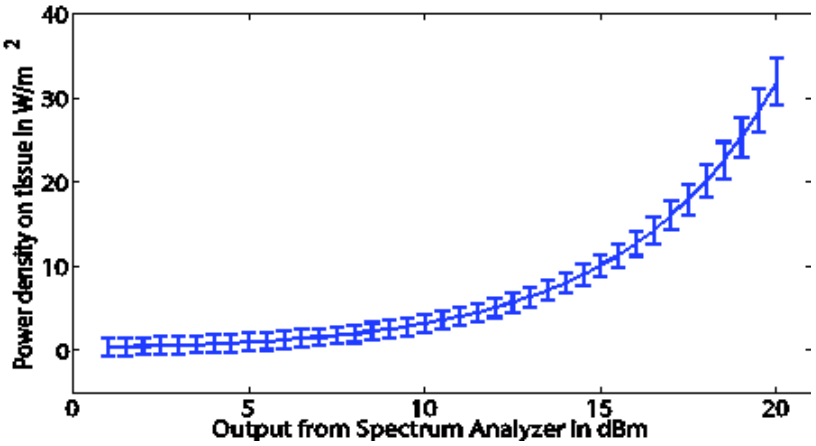

Figure 2. Uncertainty Measurements Ranging from 1-20 dBm. Uncertainty measurements for the equipment used to verify the level of RF power density exposure of the mice for a range of 1-20dBm. This graph can be compared to the IEEE standard to ensure that mice are not being exposed to higher than allowable power density levels [4].

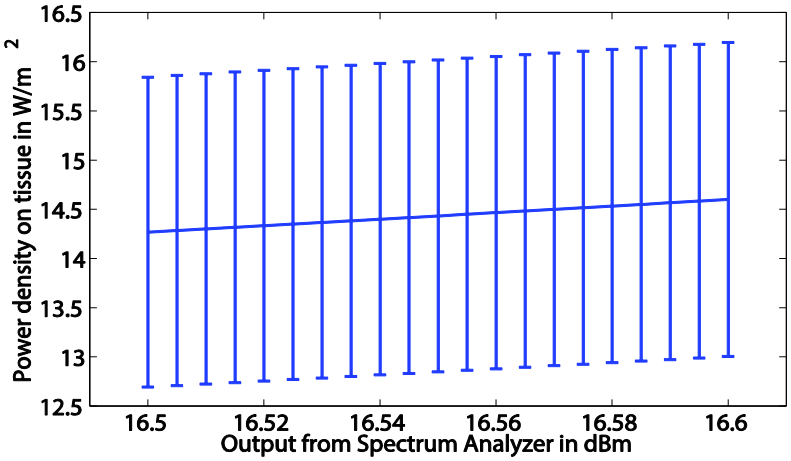

Figure 3. Uncertainty Measurements Ranging from 16.5-16.6 dBm. A close-up of the uncertainties for the range of power densities achieved when the spectrum analyzer reads in the range of 16.5-16.6 dBm. The maximum uncertainty value seen at 16.6 dBm must be less than the level recommended by IEEE for continuous exposure limits [4].

1.2.2. Uncertainty Analysis of Equipment used for Characterization of the Test Room

The spectrum analyzer has a frequency range from 9 kHz-3.0 GHz, and the biological antenna has a frequency range of 25 MHz-4 GHz. We assumed that the uncertainty values from the equipment data sheets were correct because the equipment was recently calibrated. Therefore, we calculate the power received by the spectrum analyzer as:

$$PrdB=PRba+2*|C_{l}dB| \quad (13)$$

where $PrdB$ is the power received at the spectrum analyzer, $PRba$ is the power received at the biconical antenna. Knowing the uncertainty of both the biconcial antenna and the transmission lines, we can calculate the total uncertainty as follows:

$$U_{PrdB}=\pm\sqrt{\left(\frac{\partial PrdB}{\partial PRba}*U_{PRba}\right)^{2}+\left(\frac{\partial Pr}{\partial C_{l1}}*U_{C_{l1}}\right)^{2}+\left(\frac{\partial Pr}{\partial C_{l2}}*U_{C_{l2}}\right)^{2}}. \quad (14)$$

Because the uncertainty of the transmission lines are equal, we can simplify this to:

$$U_{PrdB}=\pm\sqrt{(U_{PRba})^{2}+2*(U_{C_{l}})^{2}}. \quad (15)$$

Using the uncertainty values provided for the characterization of the test room equipment, we are able to calculate the overall uncertainty of our equipment as approximately ±1.0000 dBm.

1.2.3. Uncertainty Analysis of Equipment Used For Specific Absorption Rate Experimental Measurements

Incident power density and specific absorption rate (SAR) are commonly used to characterize RF energy exposure in the aforementioned exposure systems. Power density is the amount of power (in W) per unit area (in m^2). It can be calculated by using equation 5.

SAR is a measure of electromagnetic (EM) energy absorbed by a body. SAR calculation can be accomplished through theoretical, experimental and empirical techniques. The Radio Frequency Radiation Dosimetry Handbook (Fifth Edition) [9] describes both theoretical and experimental SAR techniques. A common theoretical SAR technique is electromagnetic (EM) simulation (e.g. COMSOL, HFSS, FDTD). Five common experimental SAR measurement techniques include:

1. Differential power measured in a closed exposure system.
2. Rate of temperature change in the biological test subject measured with noninterfering probes.
3. Calorimetric techniques.
4. Thermographic techniques.
5. Implantable E-field probes.

Finally, Durney *et al* [2] describes an empirical SAR technique. Which of these techniques are used to calculate SAR depend on the availability of resources. Using the equations found in Radio Frequency Radiation Dosimetry Handbook (Fifth Edition) 2009

$$P_e=P_I-P_O-P_R \ (W) \tag{16}$$

and

$$P_s=P_I-P_O-P_R \ (W) \tag{17}$$

where P_e is the power absorbed by the patch antenna in the empty enclosure; P_I is the input power; P_O is the output power; P_R is the reflected power; and P_s is the power absorbed by the patch antenna while the sample is present in the enclosure in Watts. After P_e and P_s are measured, the SAR is calculated by using

$$SAR=\frac{|P_e-P_s|}{m_{(subject)}}. \ (W/kg) \tag{18}$$

Then the uncertainty for SAR is:

$$U_{SAR}=\pm\sqrt{\left(\frac{dSAR}{dPe}*U_{P_e}\right)^2+\left(\frac{dSAR}{dPs}*U_{P_s}\right)^2+\left(\frac{dSAR}{dm}*U_m\right)^2}. \tag{19}$$

In Eq. 19, U_{P_e} and U_{P_s} are both equal to the uncertainty of power received at the spectrum analyzer, U_{PrdB} in Eq. 14. Using these equations, the uncertainty of the SAR measurements was found to be 0.00034216 W/kg.

1.2.4. Microstrip Patch Antenna

The microstrip patch antenna (MPA) is widely used because of its low volume and thin profile characteristics [1]. Also the microstrip antennas are inexpensive to manufacture using today's modern printed-circuit technology and versatile in terms of resonant frequency, polarization, pattern and impedance. The microstrip patch antenna is a good candidate to be used as an antenna to measure the received power and calculate the power density for safe RF exposure of mice.

1.2.5. Design and Prototyping of Rectangular Microstrip Patch Antenna

A rectangular MPA with a microstrip feed is designed so its pattern maximum is normal to the top patch surface. Next, the length and width of the radiating patch are calculated using the design equations given in [10]. The antenna is designed for the frequency of 2.43 GHz, which is in industrial, scientific and medical (ISM) radio bands. Also this is the same frequency that the mice will be exposed to using a horn antenna in a set of experiments conducted by the authors. The geometry of

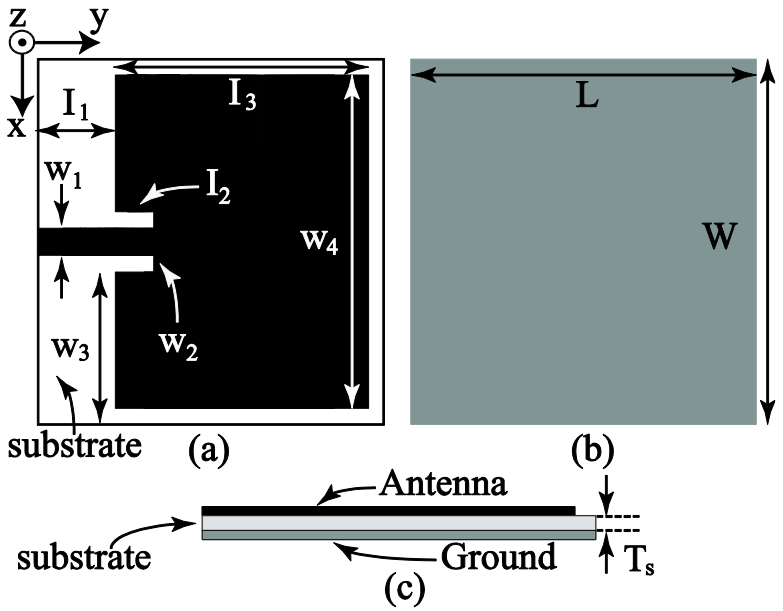

Figure 4. Geometry of the Microstrip Patch Antenna. (a) Top view. (b) Bottom view and (c) side view. Structure characteristics: l_1 = 11.8 mm, l_2 = 2 mm, l_3 = 27.5 mm, L= 50 mm, w_1 = 2.1 mm, w_2 = 1 mm, w_3 = 20.85 mm, w4 = 45 mm, W = 48.5 mm and T_s = 1.52 mm.

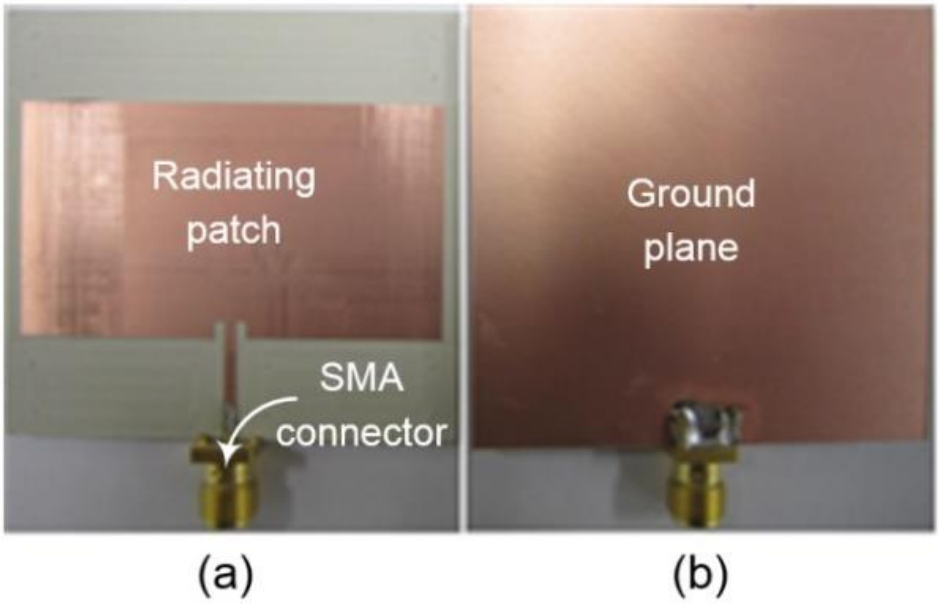

Figure 5. Fabricated Patch Antenna. Fabricated sample of the patch antenna used for measuring the power density. (a) Top view. (b) Bottom view.

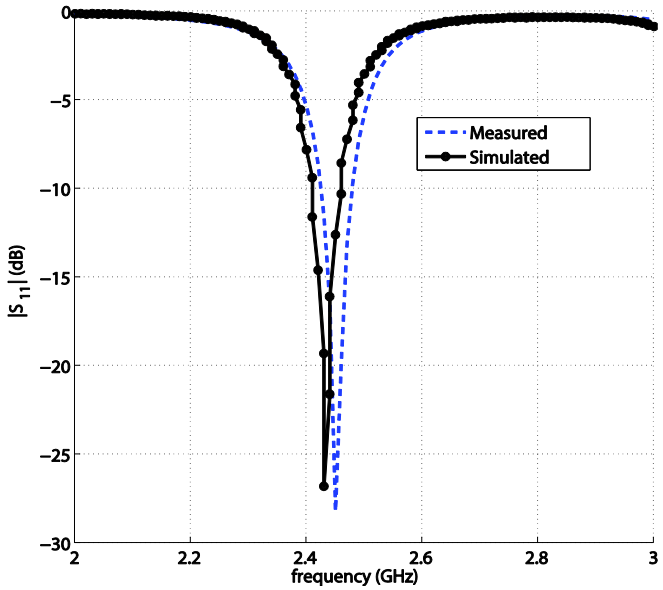

Figure 6. Patch Antenna S11 Values. Reflection coefficient S_{11} values in dB.

the MPAwith detailed dimensions are shown in Figure 4. The top layer is the radiating patch while the bottom layer is the ground plane of the antenna. As shown in the Figure 4, the actual size of the radiating patch is 27.5 x 45 mm^2 which is matched to a 50 Ω using an inset-fed microstrip line. A detailed picture of the manufactured microstrip-fed rectangular patch antenna is shown in Figure 5. To demonstrate the layout in Figure 4, a prototype was designed using TMM4 ($\varepsilon = 4.5$, $\tan\delta = 0.0020$, copper thickness = 17.5 µm, and substrate thickness/Ts = 1.52 mm), manufactured and tested. Figure 6 shows the S_{11} for the measured and simulated values.

1.2.6. Simulation and Measured Results of the MPA

All the properties of a MPA mentioned in the previous section were used in the full wave design tool, Ansoft HFSS [1], to simulate and optimize the results prior to fabrication. The simulated and measured results of the reflection coefficient are shown in the Figure 6, which shows good agreement between the simulated and measured results. A slight shift in the resonance frequency is due to the fabrication tolerance. Also these results show that the antenna is matched with a 50 Ω port. Furthermore, Figure 7 shows the measured radiation pattern of the

MPA which is broadside. The pattern shows high back radiation which is due to the small ground plane. Small ground plane was used because of good impedance matching at the resonant frequency. The antenna is linearly polarized in y-axis according to the orientation used in Figure 4.

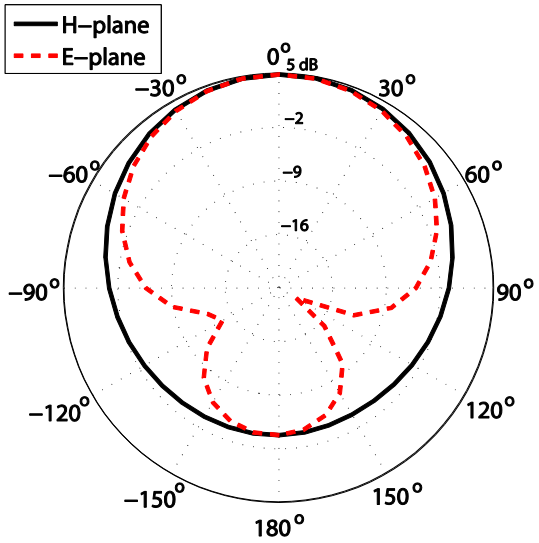

Figure 7. Measured Radiation Pattern. Measured radiation pattern in the principal xz-plane (H-plane) and yz- plane (E-plane). Spectrum analyzer is attached to a biconical antenna. The connection is made with two transmission lines, each 61 cm long connected via Agilent interconnects.

1.2.7. Characterization Of The Test Room

Before the experiment began, the radio frequency energy profile of the room was characterized on the x, y, and z-axes. This characterization process is to determine if any unwanted RF energy is present in both the test area and the control area of the mouse room. In order to characterize the RF energy, a biconical antenna is placed on a wooden tripod approximately 122 cm tall and placed in the area of the room where the control mice would reside throughout the study. The direction of the antenna coincided to the x-axis. Photographs were taken of the setup noting the position and direction of the antenna. The spectrum analyzer saved the highest recorded power using the 'Hold Maximum' function for each frequency during

the duration of the characterization process. Data were recorded for 24 hours. The experiment was then repeated, by moving the antenna to be polarized in the y- and x- axes. Finally, the process was repeated in the area where the test mice would reside throughout the RF exposure study. Trends in the RF energy can be seen at various frequencies in Figure 8 and Figure 9. The spikes are most likely caused by various electronic devices. For example, WiFi has a frequency of 2.4 GHz, and cellphone providers commonly use 0.7-0.9 GHz and 1.9 GHz bands. The change in RF energy can be caused by a wide variety of factors. For example, spikes are much more prevalent for the x-axis for the control area, most likely because the biconical antenna was pointed toward the hallway.

The increased traffic in the hallway easily could have contributed to the increased RF activity and spikes in the graph. In addition, the high spikes seen for the Z-axis for the control area could be attributed to the ductwork directly above the antenna. All values recorded during the 24 hour time period were maximum values, meaning there is no way to know how long the mice were exposed to these levels of RF energy. These energy spikes could have occurred sporadically throughout the test, or they could have remained fairly constant. However, most spikes did not exceed more than -20 dBm, which is well below the exposure power level of the treatment group. Nonetheless, it is important to limit as much unwanted RF energy as possible. Therefore, anechoic material was set up around both the test and the control mice to limit extraneous RF energy exposure. In addition, during the experiment, cellphones and other electronic devices were not allowed in the test room.

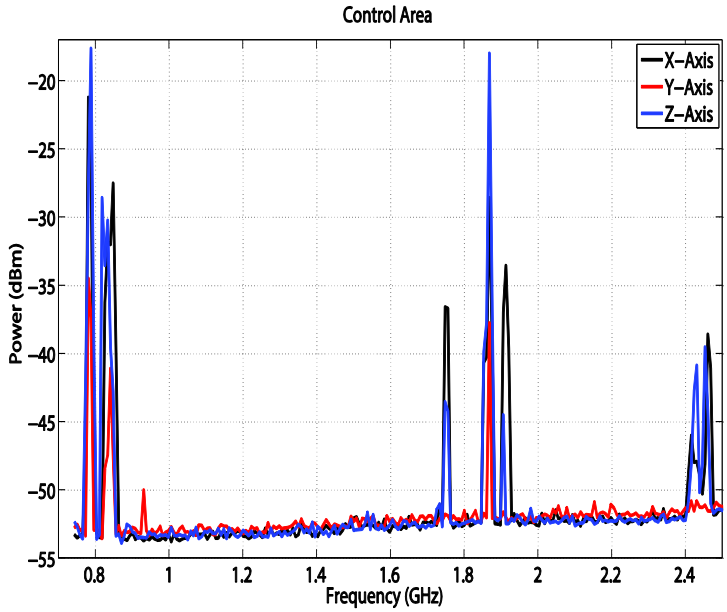

Figure 8. Noise Measurements for Control Area. Maximum RF values for the control area at frequencies of 700kHz to 2.5GHz for the control area over the 24 hour study.

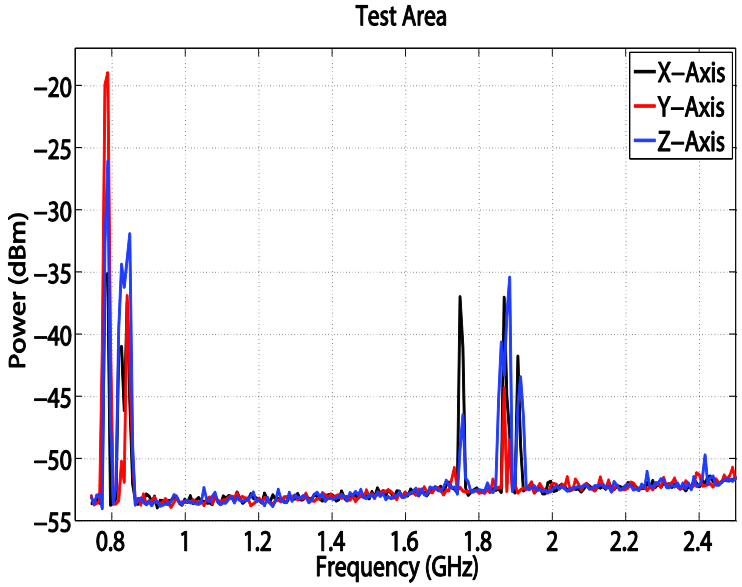

Figure 9. Noise Measurements for Test Area. Maximum RF values for the test area at frequencies of 700kHz to 2.5GHz for the test area over the 24 hour study.

1.2.8. Experimental Specific Absorption Rate Calculation

For this study the SAR was calculated using the differential-power technique and empirical calculations. Figure 10 shows the experimental setup for the SAR calculations. In short, the procedure was conducted inside an anechoic chamber to remove any outside EM noise

and provide a well-defined environment. A horn antenna connected to a power amplifier and signal generator transmitted an EM field at 2.45 GHz with a maximum power density of 1.6mW/cm^2. This power density was measured by a patch antenna located below a plastic cage and recorded by a spectrum analyzer (in dBm). A horn antenna was used to measure the reflected power at eight different locations in a circular rotation with a radius of 38.0 cm at the level of the transmit antenna (as shown in Figure 10) and recorded by a spectrum analyzer (in dBm). The average whole body SAR was measured to be 0.3422±.00034 W/kg at a maximum power density of 1.6mW/cm^2 which compares well to empirical SAR calculations using the equations found in Durney *et al.* [2], which calculates a value of 0.3750 W/kg for small animals.

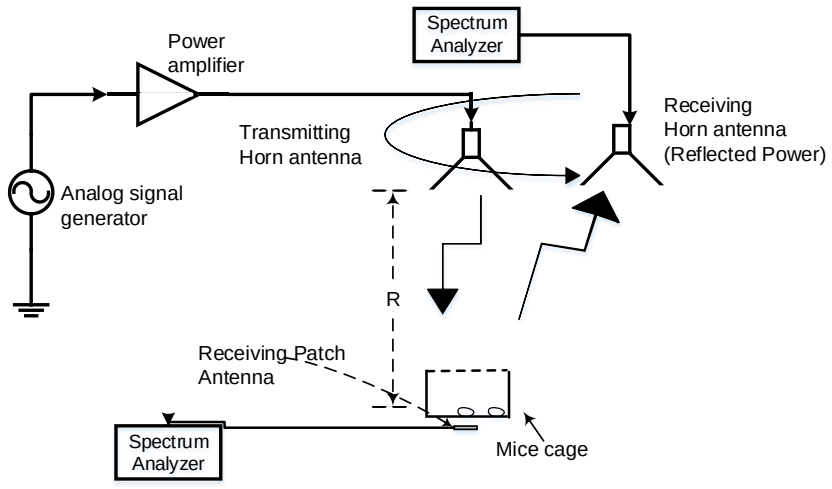

Figure 10. Specific Absorption Rate Experimental Setup. Using a horn antenna to transmit a power density of 1.6 mW/cm^2, and a patch antenna to measure the incident power. A horn antenna was used to measure the reflected power, this was conducted over eight locations ~38 cm. away from the transmitting horn antenna.

1.2.9. Example RF Exposure System Implementation

Following calibration of equipment and characterization of background, mouse cages are adopted for RF studies. This involved using non-metal cages, food trays, and water dispensers. In addition, a Plexiglas top is added with many ventilation holes (~.635 cm.) to ensure that mice

remain in their respective cages. For radio-frequency exposure experiments BALB/c mice (6-9 weeks of age) were obtained from Jackson laboratory (Bar Harbor, ME, USA). Animals were housed on Alpha-dri^{TM} paper bedding (Shepherd Speciality Papers, Watertown, TN, USA) in micro filter-topped cages (Ancare, Bellmore, NY, USA) in a specific pathogen-free facility with ad libitum access to food and water.

The mice are then separated into treatment and control groups respectively. Anechoic material is used in both the treatment and control group to limit the exposure of background RF and to ensure that the control group is not radiated with stray test RF energy. Figure 11 shows the equipment setup for the treatment group. According to the reference system used in Figure 11, the horn antenna is polarized in z-direction and receiver antenna was placed in the same direction in which the horn is polarized. Moreover, this distance 'R' is crucial for receiving safe power density at the right level i.e., top of mice body as shown in Figure 11. This distance is dependent on the frequency used, gain (G_t) of the Horn antenna and power transmitted (P_t) from the Horn antenna. Equation 20 shows the relationship:

$$Pr(dBm) = Pt\ (dBm) + Gt\ (dB) + Gr\ (dB). \tag{20}$$

This relationship is known as Friis's transmission equation [IEEE Standard, 1988]. In order to ensure that the treatment mice are receiving the correct dose of RF energy, a patch antenna connected to a spectrum analyzer was used to record the power received. This power received by the mice is below the standards set by IEEE which is 1.6 mW/cm^2 for 2.45GHz [4]. Using uncertainty analysis, RF power density levels are set and the power level within the anechoic material was also mapped to verify that the power-density levels were below maximum allowed IEEE safe exposure standards. Mice were placed within their control or treatment cages. Treatment mice can then be exposed to RF energy for a set duration.

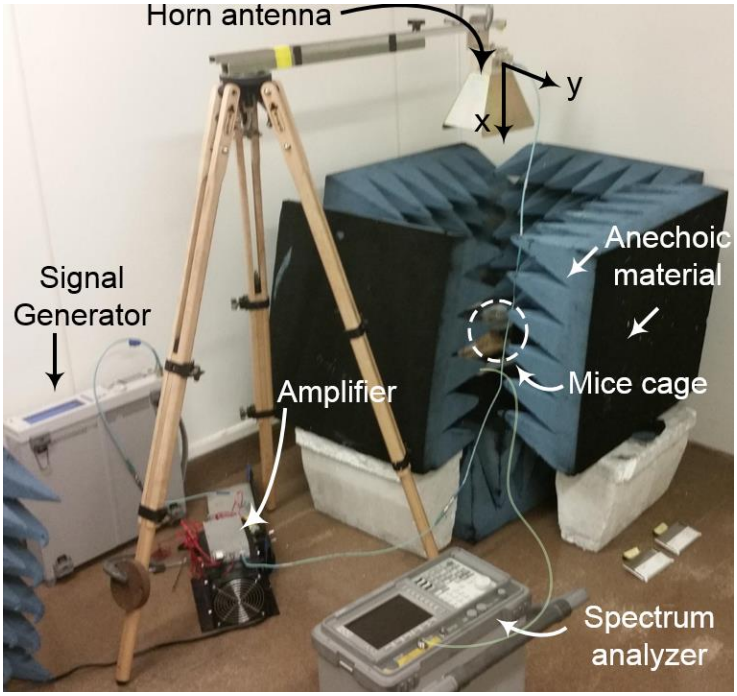

Figure 11. Photograph of the Experimental Setup for RF Exposure of Mice with All the Apparatus Used. Mice cage and patch is enclosed in the anechoic material but the horn antenna, spectrum analyzer, signal generator together with the amplifier can be seen. The horn antenna as setup in Figure 10, is polarized in the z-direction.

1.3. Discussion

This experimental exposure system can be used for repeatable long term far-field RF exposure for freely-moving mice. The equipment used promotes convenient uncertainty analysis that in turn provides more accurate power density and SAR estimates. In addition, anechoic material reduces potential environmental effects on these estimates and the steps outlined in this work can be easily changed to include many different experimental parameters (e.g. frequency, time of exposure, signal type, pulsed or continuous).

An improvement to the exposure system reported here includes an independent estimate of SAR based on full-wave electromagnetic simulations and theoretical computations on a 3D whole mouse model. This would allow for independent verification of the experimental

differential power procedure used here to estimate SAR and found in the Radio Frequency Radiation Dosimetry Handbook (Fifth Edition) [9].

1.4. References

[1] C.A. Balanis, *Antenna theory analysis and design*, 3rd ed., New York, Wiley 2005.

[2] C.H. Durney, et al. "An empirical formula for broad-band SAR calculations of prolate spheroidal models of humans and animals," *IEEE Trans Microw Theory Tech* vol. 27, pp 758–763. 1979.

[3] L. Gherardini et al., "Searching for the perfect wave: the effect of radiofrequency electromagnetic fields on cells," *Int J Mol Sci* vol.15, pp 5366–5387, Feb. 2014.

[4] International Non-Ionizing Radiation Committee of the International Radiation Protection Association. "Guidelines on limits on exposure to radio frequency electromagnetic fields in the frequency range from 100 kHz to 300 GHz." *Health Phys.* vol. 54, pp. 115-123, 1988.

[5] K.K. Kesari, et al., "Mutagenic response of 2.45 GHz radiation exposure on rat brain." *Int J Radiat Biol* vol. 86, pp.334–343, May 2010.

[6] M. Kundi, "The controversy about a possible relationship between mobile phone use and cancer." *Environ Health Perspect* vol.117, pp.316–324, Mar. 2009.

[7] A. Paffi, et al., "Microwave exposure systems for in vivo biological experiments: a systematic review." *IEEE Trans Microw Theor Tech* vol.61, pp.1980–1993, May 2013

[8] C. Polk and E. Postow, *Handbook of biological effects of electromagnetic fields*, CRC press, 1995.

[9] *Radio frequency radiation dosimetry handbook*, 5th ed., Air Force Research Lab Brooks AFB TX Human Effectiveness Directorate, TX, 2009.

[10] W.L. Stutzman and GA Thiele, *Antenna theory and design*, 2nd ed. New York, Wiley 1998.

[11] J. Vanderstaeten and L. Verschaeve, "Gene and protein expression following exposure to radiofrequency fields from mobile phones," *Environ Health Perspect* vol. 116, pp.1131–1135 Sept. 2008.

[12] S. Wasoontarajaroen, et al., "Cylindrical waveguide electromagnetic exposure system for biological studies with unrestrained mice at 1.9 GHz," *Health Phys* vol. 103, pp.268–274 Sept. 2012.

[13]*Workshop on EMF and Health Risk Research*, Switzerland, Monte Verità, Oct. 2012.

PAPER 2. THE EFFECTS OF 2.45 GHZ RADIO FREQUENCY ENERGY ON HEART TISSUE GENES USING AN UNRESTRAINED MURINE MODEL *IN VIVO*[1]

2.1. Introduction

Radio frequency (RF) energy is widely used in technologies such as Wi-Fi, Bluetooth, and other wireless devices. As the use of RF energy continues to grow, there has been a rising concern on how RF energy affects the body. Notably, it has been shown that RF energy above certain power densities has the potential to cause genetic changes, heating, and ablation of tissue. To avoid this, safe levels of exposure have been developed (IEEE, WHO), however, research on safe levels of RF energy on the body remain controversial and inconclusive [4, 5, 12, 15, 18].

These controversies are due to five key variances in experimental protocols and analysis of results, namely: exposure systems, using restrained vs. unrestrained subjects, using in vivo vs. in vitro samples, differential gene expression quantification techniques, and statistical analysis approaches. Furthermore, a major difference in experimental exposure systems are those that bathe the whole body versus those that localize exposure to a specific organ. A downside of the latter is the potential lack of interaction between organ systems. In addition to differences in exposure systems, studies can vary between restrained and unrestrained subjects [13]. While restrained subjects' exposure is constant throughout the study, a potential side effect is the upregulation of stress-related genes [2]. Though in vitro samples lack the need for restraint there

[1] The material in this chapter was co-authored by Jared Hansen, Brandon Stevens, Sajid Asif, Lauren Singelmann, Muhammad Khan, Sumit Ghosh, Tom Gustad, Curt Doetkott, Benjamin Braaten, and Daniel Ewert. Jared Hansen performed the experiment, analyzed the heart results and co-wrote the paper. Brandon Stevens performed the experiment, analyzed the brain results and co-wrote the paper. Sajid Asif built the patch antenna and help setup and build the experiment. Lauren Singelmann helped build the experiment and helped with RNA isolation. Muhammmad Khan worked on the microstrip patch antenna. Sumit Ghosh assisted in RNA isolation, animal care, and supervised the experiment. Curt Doetkott built the statistical methods and assisted in supervising the data analysis. Tom Gustad helped in animal care and supervision of the study, Benjamin Braaten, and Daniel Ewert supervised the experiments and provided review feedback.

is concern these samples lack cell-to-cell interaction that in vivo tissue samples exposed to RF energy experience [16].

In addition to the varying experimental techniques, the process of analyzing gene expressions can impact findings. The two most common gene analysis procedures are qPCR and microarray analysis, but both of these methods have shortcomings. While qPCR is very accurate, only a small sub-section of genes can be analyzed. Conversely, microarray analysis allows evaluation of the full genome, but there is concern about the accuracy of the measurements as stated by [17].

Once gene expression is analyzed, a statistical method must be used to compare findings. Generally, statistical methods fall into two types, parametric and nonparametric testing. Parametric tests assumes a probability distribution e.g. Student's t-test, F-test, etc. The downfall of parametric testing is the data may not fall under the assumed distribution. Therefore, researchers have investigated nonparametric testing. One common type is log-rank test that use the sum of ranks between the test and control populations. These tests work well for low population data, but assume underlying test and control distributions are similar in shape [1].

Statistical permutations and combinations are two types of nonparametric testing. Statistical permutations builds a reference distribution from each sample. This process can be computationally involved for large sample data sets. Unlike permutations, statistical combinations require less computation time to build a complete distribution, therefore. Using combinations is identical to the use of permutation to build a distribution.

The objective of this study is to determine if safe levels of RF energy alter gene expression in a murine model in vivo. In order to determine gene alteration on a whole genome basis, RNA-Seq is used to analyze genes. RNA-Seq allows full genome analysis while providing

accuracy analogous to qPCR [11, 18, 20]. In addition, the manuscript describes a different nonparametric test using combinations to build distributions. These distributions are used to establish empirical p-values for each transcription.

This manuscript describes a 31 day experiment with whole body exposure to continuous RF energy at 2.45 GHz on unrestrained, in vivo subjects. Using RNA-Seq to analyze the entire murine genome, the data are statistically analyzed using combinations and empirical p-values. Data were analyzed through the use of QIAGEN's Ingenuity® Pathway Analysis (IPA®, QIAGEN Redwood City, www.qiagen.com/ingenuity). This experiment sheds light onto the effects RF energy has on the mouse genome in brain and heart tissue.

2.2. Methods

2.2.1. Parameters

Table 3 depicts the experimental parameters used for this study. The uncertainty values and justification of the parameters can be found in [7].

Table 3
Test Parameters

No	Parameter	Value
1.	Frequency	2.45 GHz
2.	Power Density	1.434±0.159 mW/cm^2
3.	Specific Absorption Rate	0.3422±0.0003 W/kg (Average Whole Body)
4.	Signal Type	Continuous Sinusoid
5.	Time of Exposure	31 Days
6.	Ntest	11 Mice
7.	Ncontrol	11 Mice

2.2.2. Selection of Species

BALB/c mice (6-9 weeks of age) were obtained from Jackson laboratory. Animals were housed on Alpha-dri^{TM} paper bedding in micro filter-topped cages in a specific pathogen-free facility with access to food and water ad libitum.

2.2.3. Experimental Setup

The complete experimental setup and justifications can be found in Hansen *et al* [7]. Briefly, the horn antenna is placed a distance 52 cm above the plastic mice cages then connected to a signal generator and power amplifier. Figure 1 shows the experimental exposure setup. A patch antenna is placed near the cages to measure the power density throughout the study. Due to cage size restrictions the experiment is split into two, 31 day studies.

2.2.4. Radio Frequency Exposure Experiment

Mice were continuously exposed to RF energy at 2.45 GHz frequency at a power density of 1.434±0.159 mW/cm^2 for 31 days. Control mice were placed in similar test systems without exposure to the RF energy. The mice were observed daily to ensure heating from RF energy was not occurring. After the first 31 days, this protocol was repeated for other test and control mice until the total number of mice in both groups was eleven.

2.2.5. Tissue Extraction

Following an approved IACUC protocol the mice were euthanized using CO_2 asphyxiation and readied for tissue extraction [9]. The process of tissue extraction followed "Guide to Necropsy of the Mouse" [3]. After tissue was extracted from the control and test groups they were flash frozen in liquid nitrogen and stored at -80˚C.

2.2.6. Tissue Analysis Methods

Tissue was analyzed using the methods described in Ghosh *et* al [6]. Briefly, the RNA was isolated from tissue using Phenol-chloroform extraction. TRIzol was used in a homogenized sample to separate the RNA. The samples then received alcohol precipitation to further purify the concentration of RNA. As a quality check for contamination and concentration, the quality and purity of the samples were tested using a Nanodrop. Samples with concentrations and purity below RNA-Seq standards were excluded for the analysis e.g. samples had to have concentrations greater than 200 ng/µL and 260/280 purity greater than 1.9. After RNA isolation was completed for the samples, they were sent to an outside core facility, Genome Technology Access Center in the Department of Genetics at Washington University School of Medicine (GTAC) to undergo RNA-Seq.

2.2.7. Data Analysis

TPM (transcripts per million) values were used for analysis for each transcript; the values were statistically analyzed in SAS®. When all subjects had zero TPM values, these transcripts were removed from the statistical analysis. The test statistic is defined in equation 21,

$$stat_t = \frac{\frac{\sum_{i=1}^{n_{test}} TPM_{test}}{n_{test}} - \frac{\sum_{i=1}^{n_{control}} TPM_{control}}{n_{control}}}{\frac{\sum_{i=1}^{n_{test\ and\ control}} TPM_{test\ and\ control}}{n_{test\ and\ control}}}. \quad (21)$$

This variable, $stat_t$, was used to build a density distribution for all transcripts. Figure 12 shows the density distribution for the heart data. As seen in Figure 12, there are high densities at stat extremes e.g. ±2. To determine if these high densities were not random error the data was arbitrarily filtered and the distributions were shown again in Figure 13. To determine if these extremes and other samples are statistically significant, empirical p-values must be computed. In

order to obtain empirical p-values for individual transcripts, transcript level distributions are built using statistical combinations without replacement (Eq. 22) [10].

$$\binom{n}{k}=\frac{n!}{k!(n-k)!} \tag{22}$$

For equation 22 k is the size of the test group and n is the total amount of subjects in the data set. To build the entire density distribution with combinations the n choose k TPM values were placed into the test group and their complements were placed into control group. Equation 21 was also used to calculate the variable $stat_c$ for each generated combination.

Empirical p-values were calculated for each transcript's statistical combination distribution using equations 23,

$$P_{comb}=\frac{\sum_{1}^{\binom{n}{k}}(stat_c \geq stat_t)}{\binom{n}{k}} \tag{23}$$

Explanation for this equation can be found in [8, 11].

In IPA, each data set was separated into heart and brain organ systems. P-value percentiles were found for heart and brain. Figure 14 shows the empirical cumulative distribution plot for the heart. The plot shows the percentile for each corresponding empirical p-value. In IPA the pathways, diseases and functions were explored. Table 4 describe the disease and functions that were impacted and the amount of genes that have p-values that are less than 0.05 for heart tissue.

2.3. Results

Due to concentration and purity issues during RNA isolation, seven test and seven control subjects were able to be quantified using RNA-Seq for heart data. Data analysis was conducted for these sequenced samples.

As expected large densities of $stat_t$ values are found near the distribution mean. Indicating that most transcripts were unaffected by RF energy. Also as expected densities decrease at larger stat values. Unexpectedly, large densities found near the maximum and minimum stat values in Figure 12, in order to determine if the extremes were caused by random error a new distribution was created using arbitrarily filtered data for amount of non-zero subject per transcript. Figure 13 shows distributions for heart data filtered for non-zero values in >4 subjects. This is solely to determine how many extremes fall outside of the filter, and the filter was only used for that distribution. The bins are set to 500 in order to better interpret the results.

P-values for the heart system can be found in Figure 14. For heart data 10.20% of genes were found to have p-values of <0.05. Table 4 lists the functions and diseases effected, the number of genes with p-values below 0.05, and the number of genes with $stat_t$ extremes.

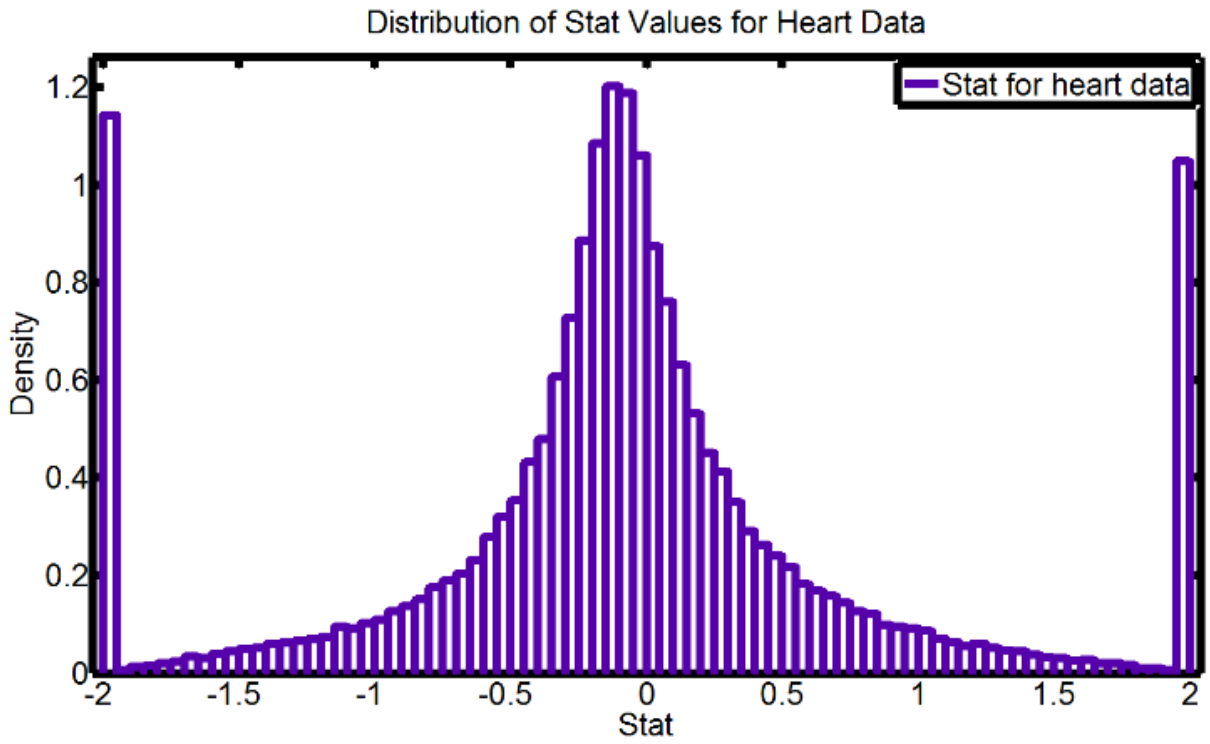

Figure 12. Stat Value Distribution. The mean for the stat values is -0.076. The peaks found at ±2 are attributed to values where average test TPM values are non-zero and average control TPM values are zero (+2) or *vice versa* for (-2).

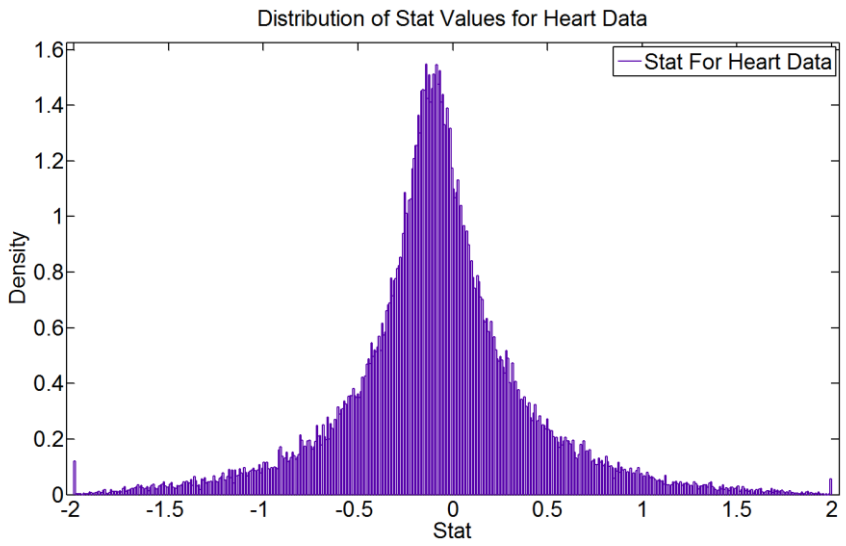

Figure 13. Filtered Stat Value Distribution. Distribution for heart data filtered for non-zero values in >4 subjects. The mean for the stat values is -0.084. 500 bins are used in order to better interpret the results.

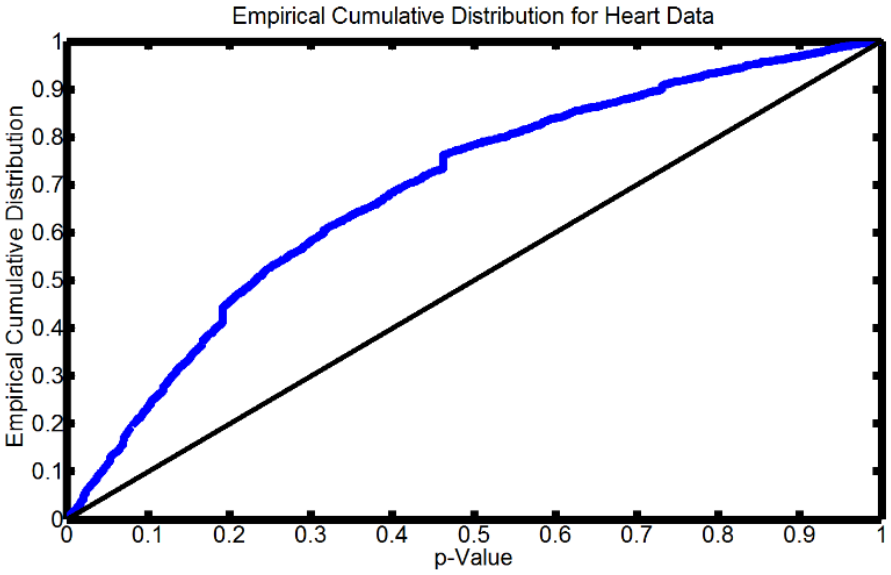

Figure 14. Empirical Cumulative Distribution. The empirical cumulative distribution for heart data filtered for organ system in IPA. The percentage of p-values found below 0.05 is 10.20%. The amount of genes with p-values below 0.05 is more than 5% of the total genes analyzed. Meaning, the percentage is above standard error. The percentages are above standard error showed by black line. If all p-values were equally likely, then the empirical cumulative distributions would be the same as the black line, meaning no effect would exist.

Table 4
Disease or Function

No	Disease or Function	Number of Genes with p-value <0.05	Number of Genes with Extreme stat Values
1	Hypertrophy of heart	24	2
2	Cell death of cardiomyocytes	11	2
3	Hypertrophy of heart cells	8	0
4	Dysfunction of heart	7	2
5	Damage of heart	6	2
6	Hypertrophy of cardiac muscle	6	0
7	Ventricular hypertrophy	6	0
8	Injury of heart	5	2
9	Hypertrophy of cardiomyocytes	4	0
10	Failure of heart	4	1
11	Proliferation of cardiomyocytes	4	0
12	Hypertrophy of left ventricle	4	0
13	Coronary artery disease	3	1
14	Myocardial infarction	3	1
15	Hypertrophy of right ventricle	3	1
16	Dilation of heart	3	2
17	Hypoplasia of trabeculae carne	3	0
18	Fibrosis of coronary artery	2	0
19	Transformation of endocardial cells	2	0
20	Cardiac output of heart	2	1
21	Stenosis of aortic valve	2	0
22	Diastolic dysfunction of heart	2	0
23	Dilation of left ventricle	2	0
24	Cardiac fibrosis of heart tissue	1	1
25	Perivascular fibrosis of coronary artery	1	1
27	Atherosclerosis of coronary	1	0
28	artery	1	0
29	Injury of heart tissue	1	0
30	Hypertrophy of coronary artery	1	1
31	Hypertrophy of heart septum	1	0
32	Stenosis of pulmonary valve	1	1
33	Reperfusion injury of heart	1	0
34	Degeneration of cardiomyocytes	1	0
35	Hypertrophy of myocardium Inflammation of heart	1	1

2.4. Discussion

Most genes were unaffected by RF energy as shown by high density of $stat_t$ values near the distribution mean, in Figure 12. Also, the density values of $stat_t$ decrease rapidly from the distribution mean. Unexpectedly, high densities were found at the stat extremes found in both Figure 13. This is attributable to transcripts where TPM expression values are found in the test group and not the control group (or *vice-versa*). Maximum and minimum $stat_t$ values occur when the mean of the control group has a zero value (maximum) and the test mean is non-zero, or the mean of the test group has a zero value and the control mean is non-zero (minimum). Expressed another way, some transcripts that were "off" in the control group were switched "on" in the test group. Conversely, some transcripts were normally "on" in the control group and were switched "off" in the test group.

These unique findings are potentially suggestive of RF energy's ability to "switch on" or "switch off" certain genes, in other words RF energy may activate genetic control switches in a digital on/off response. Related to the digital behavior, other transcripts were found to be significantly up or down regulated by RF energy. Modulation of genetic expression levels is suggestive of an analog response to RF energy. Analog behavior is a modulation of the expression rate, but not to the extent of turning on or off a transcript. Our statistical approach produced high p-values when only a few subjects showed transcript expression with in a group. For example, all control subjects had TPMs of zero and a few of the test subjects showed TPM values that were non-zero. In this example the $stat_t$ was found to not be statistically significant. Figure 13 shows distributions for data sets filtered for non-zero values in >4 subjects for heart data and Figure 13 show that the densities near the max and min remain. The densities are decreased, yet are still larger than densities near them.

In Figure 14 the empirical cumulative distributions were calculated for each organ system. The percentage of transcripts with p-values <0.05 are much higher than the 5% random error and in both cases are more than double the percentage. Though both of the percentages are higher than 0.05 it should be noted that type-one error was not reduced using something such as a False Discovery Rate (FDR). This is due to the sample size limitations and the use of empirical p-values and statistical combinations. With the total sample size of 14 for this data set, the lowest p-value would be ~1/3400. Where the ~3,400 is the result of the 14 choose 7. With the amount of transcripts above 70,000, a large sample size would need to be used to use an FDR on that amount of data. An increase in subjects will give the ability to reduce the possibility of type one error using an FDR.

Table 4 shows the disease and function impacted by RF energy. For both tables the amount of organ system related function is high, and in many cases have a large percentage of genes associated with that function altered. Investigation into the genes altered for each functional group are associated with both positive and negative impact. Meaning, no conclusion can be drawn on the potentially malicious or aiding nature of RF energy. Future studies will need to be conducted to: 1. Recreate the results found in these disease and functions, 2. Explore the genes involved in the functional groups, 3. Investigate if the functions are also affected in disease murine models and 4. Explore the underlying cellular mechanisms and their interaction with RF.

2.5. Conclusion

This thesis described a 31 day experiment with whole body exposure to continuous RF energy at 2.45 GHz on unrestrained, in vivo subjects. The first paper describes an experimental exposure procedure which allows for proper experimental technique. The second paper describes the study conducted using the procedure from the first paper, and the results suggest evidence

that RF energy altered gene expression in vivo. In addition, the interaction between RF energy and RNA response as a digital system. The impact that this genetic alteration has on cellular function is still unknown. Future studies will need to be conducted to: 1. Reproduce the results found in this manuscript. 2. Understand better the cellular mechanisms and their interactions with RF energy.

2.6. References

[1] J. M. Bland and D. G. Altman, "The logrank test," Brit Med J vol.328, pp 1073, Apr. 2004.

[2] T. Buerge and T. Weiss, "Handling and restraint," in *The Laboratory Mouse*, H. J. Hedrich and G. Bullock. Amsterdam; Boston: Elsevier Academic Press, 2004.

[3] V. Covelli, "Guide to the necropsy of the mouse," 2013.

[4] A.F. Fragopoulou, et al., "Brain proteome response following whole body exposure of mice to mobile phone or wireless DECT base radiation." *Electromagn Biol Med*, vol. 31 pp.250- 274. Jan. 2012

[5] L.Gherardini, et al., "Searching for the Perfect Wave: The Effect of Radiofrequency Electromagnetic Fields on Cells," *Int J Mol Sci* vol.15, pp. 5366-5387, Feb. 2014.

[6] S. Ghosh, et al., "B lymphocytes regulate airway granulocytic inflammation and cytokine production in a murine model of fungal allergic asthma," *Cell Mol Immunol*, Nov. 2014.

[7] J.W. Hansen, et al., "A Far-Field Radio-Frequency Experimental Exposure System with Unrestrained Mice," *SpringerPlus*, vol. 4, pp. 669, Nov. 2015

[8] T. A. Knijnenburg, et al., "Fewer permutations, more accurate P-values," *Bioinformatics*, vol. 25, pp. i161-i168. Jun. 2009

[9] S. Leary, et al., "AVMA guidelines for the euthanasia of animals: 2013 edition," Jan. 2013

[10] B. F. Manly, *Randomization, bootstrap and Monte Carlo methods in biology*, vol. 70, Boca Raton, FL. CRC Press. 2006.

[11] J. C. Marioni, et al., "RNA-seq: an assessment of technical reproducibility and comparison with gene expression arrays," *Genome Res*, vol. 18, pp. 1509-1517, Jun. 2008.

[12] J. P. McNamee and V. Chauhan, "Radiofrequency Radiation and Gene/Protein Expression: A Review." *Radiat. Res*, vol. 172, pp. 265–287, Sept. 2009.

[13] B. V. North, et al., "A Note on the Calculation of Empirical P Values from Monte Carlo Procedures." *Am J Hum Genet*, vol. 71, pp. 439–441. Aug.2002

[14] A. Paffi, et al., "Microwave exposure systems for in vivo biological experiments: a systematic review." *IEEE Trans Microw Theor Tech* vol.61, pp.1980–1993, May 2013

[15] F. Poulletier de Gannes, et al., "Report on the analysis of risks associated to exposure to EMF: in vitro and in vivo (animals) studies." *Efhran.* Jul. 2010.

[16] S. S. Rothman, *Lessons from the living cell: The limits of reductionism*. New York, McGraw-Hill Companies, 2002.

[17] T. Sakurai, et al., "Genomic architecture of autism spectrum disorders," in: *Textbook of Autism Spectrum Disorders,* E. Hollander, et al., Washington, DC: American Psychiatric Publishing, pp. 281–298. 2011.

[18] C. Trapnell, et al., "Differential analysis of gene regulation at transcript resolution with RNA-seq," *Nat Biotechnol,* vol. *31*, pp. 46-53, Dec. 2012.

[19] J. Vanderstraeten and L. Verschaeve, "Gene and protein expression following exposure to radiofrequency fields from mobile phones," *Environ Health Perspect,* vol. 116, pp.1131–1135 Sept. 2008.

[20] Z. Wang, et al., "RNA-Seq: a revolutionary tool for transcriptomics," *Nat Rev Genet*, vol. *10*, pp. 57-63. Jan. 2009.